Inorg. Chem. **2007**, *46*, 3136–3143

Two-Dimensional Iron(II) Spin Crossover Complex Constructed of Bifurcated NH···O^- Hydrogen Bonds and π–π Interactions: $[Fe^{II}(HL^{H,Me})_2](ClO_4)_2 \cdot 1.5MeCN$ ($HL^{H,Me}$ = Imidazol-4-yl-methylidene-8-amino-2-methylquinoline)

Hiroaki Hagiwara,[†] Shingo Hashimoto,[†] Naohide Matsumoto,*[,†] and Seiichiro Iijima[‡]

Department of Chemistry, Faculty of Science, Kumamoto University, Kurokami 2-39-1, Kumamoto 860-8555, Japan, and National Institute of Advanced Industrial Science and Technology, Tsukuba 305-8566, Japan

Received October 12, 2006

A 2D iron(II) spin crossover complex, $[Fe^{II}(HL^{H,Me})_2](ClO_4)_2 \cdot 1.5MeCN$ (**1**), was synthesized, where $HL^{H,Me}$ = imidazol-4-yl-methylidene-8-amino-2-methylquinoline. **1** showed a gradual spin transition between the HS ($S = 2$) and LS ($S = 0$) states from 180 to 325 K within the first warming run from 5 to 350 K, in which 1.5MeCN is removed, and there was an abrupt spin transition at $T_{1/2\downarrow} = 174$ K in the first cooling run from 350 to 5 K. Following the first cycle, the compound showed an abrupt spin transition at $T_{1/2\uparrow} = 185$ K and $T_{1/2\downarrow} = 174$ K with 11 K wide hysteresis in the second cycle. The crystal structures of **1** were determined at 296 (an intermediate between the HS and LS states) and 150 K (LS state). The structure consists of a 2D extended structure constructed of both the bifurcated NH···O^- hydrogen bonds between two ClO_4^- ions and two neighboring imidazole NH groups of the $[Fe^{II}(HL^{H,Me})_2]^{2+}$ cations and the π–π interactions between the two quinolyl rings of the two adjacent cations. Thermogravimetric analysis showed that solvent molecules are gradually eliminated even at room temperature and completely removed at 369 K. Desolvated complex **1′** showed an abrupt spin transition at $T_{1/2\uparrow} = 180$ K and $T_{1/2\downarrow} = 174$ K with 6 K wide hysteresis.

Introduction

Spin crossover (SC) is a representative example of molecular bistability in which the high-spin (HS) and low-spin (LS) states are interconvertible by physical perturbations such as a change in temperature, pressure, an external magnetic field, or light irradiation.[1,2] Whereas SC behavior is essentially a phenomenon of individual molecules, the interaction between the SC sites is an important factor governing SC properties such as the steepness and multistep nature of the spin transition, hysteresis, and LIESST (light-induced excited spin state trapping) effect, which are important properties with regard to applications in information storage, molecular switches, and visual displays.[3] The synthesis of SC compounds exhibiting interactions between the SC sites is of current interest. During the last two decades, polymeric SC compounds with bridging ligands[4] and mononuclear SC compounds exhibiting intermolecular interactions such as hydrogen bonding and $\pi-\pi$ stacking[5] have been

* To whom correspondence should be addressed. E-mail: naohide@aster.sci.kumamoto-u.ac.jp. Fax: +81-96-342-3390.

[†] Kumamoto University.

[‡] National Institute of Advanced Industrial Science and Technology.

(1) (a) König, E. *Prog. Inorg. Chem.* **1987**, *35*, 527−623. (b) Goodwin, H. A. *Coord. Chem. Rev.* **1976**, *18*, 293−325. (c) Gütlich, P.; Hauser, A.; Spiering, H. *Angew. Chem., Int. Ed. Engl.* **1994**, *33*, 2024−2054. (d) Spin Crossover in Transition Metal Compounds I-III. In *Topics in Current Chemistry;* Gütlich, P.; Goodwin, H. A., Eds.; Springer: New York, 2004; pp 233−235.

(2) (a) Decurtins, S.; Gütlich, P.; Köhler, C. P.; Spiering, H.; Hauser, A. *Chem. Phys. Lett.* **1984**, *105*, 1−4. (b) Gütlich, P.; Garcia, Y.; Woike, T. *Coord. Chem. Rev.* **2001**, *219*−*221*, 839−879. (c) Hauser, A. *J. Chem. Phys.* **1991**, *94*, 2741−2748.

(3) (a) Kahn, O.; Martinez, J. C. *Science* **1998**, *279*, 44−48. (b) van Koningsbruggen, P. J.; Garcia, Y.; Kahn, O.; Fournes, L.; Kooijman, H.; Spek, A. L.; Haasnoot, J. G.; Moscovici, J.; Provost, K.; Michalowicz, A.; Renz, F.; Gütlich, P. *Inorg. Chem.* **2000**, *39*, 1891−1900. (c) Real, J. A.; Andres, E.; Munoz, M. C.; Julve, M.; Granier, T.; Bousseksou, A.; Varret, F. *Science* **1995**, *268*, 265−267.

(4) (a) Garcia, Y.; Kahn, O.; Rabardel, L.; Chansou, B.; Salmon, L.; Tuchagues, J. -P. *Inorg. Chem.* **1999**, *38*, 4663−4670. (b) Breuning, E.; Ruben, M.; Lehn, J. -M.; Renz, F.; Garcia, Y.; Ksenofontov, V.; Gütlich, P.; Wegelius, E.; Rissanen, K. *Angew. Chem., Int. Ed.* **2000**, *39*, 2504−2507. (c) Moliner, N.; Munoz, C.; Letard, S.; Solans, X.; Menendez, N.; Goujon, A.; Varret, F.; Real, J. A. *Inorg. Chem.* **2000**, *39*, 5390−5393.

10.1021/ic061960a CCC: $37.00
Published on Web 03/16/2007

extensively investigated, and they have shown interesting SC behaviors.

We have reported the metal complexes of polydentate ligands containing imidazole groups.[6,7] Of these, iron complexes with polydentate ligands derived from the condensation reaction of 4-formylimidazole derivatives and various polyamines such as tris(2-aminoethyl)amine, bis(3-aminopropyl)ethylenediamine, 2-aminoethylpyridine, and *N*-phenylethylenediamine have been found to be a new family of SC complexes. These iron complexes assume various types of 1D and 2D extended network structures constructed by using the various types of hydrogen bonds such as the imidazole−imidazolato hydrogen bond (NH···N), NH···Cl^-, and NH···π, and they showed a variety of SC behaviors, such as gradual, steep, and multistep SC. These results demonstrated that this family of iron complexes has fascinating features giving a variety of assembly structures and multistep SC behaviors, but unfortunately these complexes generally did not show wide hysteresis. However, wide thermal hysteresis has been found in SC complexes with $\pi-\pi$ stacking interactions,[5] such as $[Fe^{III}(pap)_2]ClO_4 \cdot H_2O$,[5a] $[Fe^{III}(qsal)_2]NCSe \cdot MeOH$,[5b] and $[Fe^{II}(bzimpy)_2](ClO_4)_2 \cdot 0.25H_2O$[5f] (Hpap = 2-hydroxyphenyl-(2-pyridyl)methaneimine, Hqsal = *N*-(8-quinolyl)salicylaldimine, bzimpy = 2,6-bis(benzimidazol-2-yl)pyridine). Thus, it can be anticipated that iron complexes with a ligand involving an imidazole group and $\pi-\pi$ interactions can produce wide hysteresis and a variety of SC behaviors.

In this work, we have designed the tridentate ligand imidazol-4-yl-methylidene-8-amino-2-methylquinoline (Chart 1, hereafter abbreviated as $HL^{H,Me}$), which consists of an imidazole group that can give a hydrogen-bonded network structure and a quinoline group that can produce $\pi-\pi$ interaction. Iron(II) complex $[Fe^{II}(HL^{H,Me})_2](ClO_4)_2 \cdot 1.5MeCN$ (**1**) was synthesized and characterized by an X-ray single-crystal study, the temperature dependences of the magnetic susceptibilities, Mössbauer spectroscopy, and TGA measurement. As anticipated, the complex assumed a 2D extended structure constructed of both the bifurcated NH···O^- hydrogen bonds between the imidazole group of the complex cation and the ClO_4^- ion and the $\pi-\pi$ interactions between the quinolyl rings of the adjacent complex cations and showed an abrupt spin transition with hysteresis. We report how the coexistence of bifurcated hydrogen bonds and $\pi-\pi$ interactions can significantly affect SC behavior and the solvent molecule effect on SC behavior.

Chart 1. Schematic Drawing of $[Fe^{II}(HL^{H,Me})_2]^{2+}$.

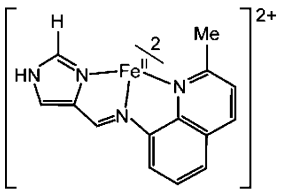

Results

Synthesis and Characterization of $[Fe^{II}(HL^{H,Me})_2](ClO_4)_2 \cdot 1.5MeCN$ (1). We note that $[Fe^{II}(HL^{H,Me})_2](ClO_4)_2 \cdot 1.5MeCN$ (**1**) was synthesized in air. The tridentate ligand was prepared by the 1:1 condensation reaction of 4-formylimidazole and 8-amino-2-methylquinoline in methanol, and the resulting ligand solution was used for the synthesis of the complex. The complex was prepared by mixing the methanol solution of the tridentate ligand and $Fe^{II}(ClO_4)_2 \cdot 6H_2O$ in a 2:1 molar ratio. Crude products were precipitated, collected by suction filtration, and recrystallized from acetonitrile. Well-grown crystals involving solvent molecules were obtained from slow crystallization at room temperature. The formula of $[Fe^{II}(HL^{H,Me})_2](ClO_4)_2 \cdot 1.5MeCN$ (**1**) was confirmed by elemental analysis and TGA measurement. The infrared (IR) spectra showed a characteristic band at 1609 cm^{-1}, assigned to the C═N stretching vibration of the Schiff base ligand. The complex showed thermochromism from black at ambient temperature to dark green at liquid-nitrogen temperature and to dark brown at about 80 °C.

Thermogravimetric data was measured to reveal the removing temperature of the solvent molecule in air. When 11.095 mg of powdered sample was heated at a rate of 1 °C min^{-1}, a two-step weight loss was observed (Caution paragraph in Experimental Section), and the total weight loss was 8.1% in agreement with the calculated weight percent of 1.5 acetonitrile (MeCN) molecules per $[Fe^{II}(HL^{H,Me})_2](ClO_4)_2 \cdot 1.5MeCN$ (**1**) (7.8%). In this two-step weight loss, a 2.7% weight loss corresponding to 0.5MeCN (2.6%) was observed in the first desolvation process at 23−41 °C (296−314 K), and a subsequent 5.4% weight loss corresponding to 1.0MeCN (5.2%) was observed at 41−96 °C (314−369 K). At the temperature closer to the boiling point of acetonitrile (81.6 °C, 354.6 K), 1.5MeCN molecules are perfectly removed, demonstrating that the solvent molecules do not interact with the rest of the molecule through any chemical bonds. Even at room temperature (28 °C, 301 K), the freshly prepared sample of **1** loses more than 1.0MeCN

(5) (a) Hayami, S.; Gu. Z.; Shiro, M.; Einaga, A.; Fujishima, A.; Sato, O. *J. Am. Chem. Soc.* **2000**, *122*, 7126−7127. (b) Hayami, S.; Gu. Z.; Yoshiki, H.; Fujishima, A.; Sato, O. *J. Am. Chem. Soc.* **2001**, *123*, 11644−11650. (c) Dorbes, S.; Valade, L.; Real, J. A.; Faulmann, C. *Chem. Commun.* **2005**, 69−71. (d) Zhong, Z. J.; Tao, J.-O.; Yu, Z.; Dun, C.-Y.; Liu, Y.-J.; You, X.-Z. *J. Chem. Soc., Dalton Trans.* **1998**, 327−328. (e) Létard, J-F.; Guionneau, P.; Codjovi, E.; Lavastre, O.; Bravic, G.; Chasseau, D.; Kahn, O. *J. Am. Chem. Soc.* **1997**, *119*, 10861−10862. (f) Boca, R.; Boca, M.; Dihan, L.; Falk, K.; Fuess, H.; Haase, W.; Jarosciak, R.; Papankova, B.; Renz, F.; Vrbova, M.; Werner, R. *Inorg. Chem.* **2001**, *40*, 3025−3033.

(6) (a) Yamada, M.; Hagiwara, H.; Torigoe, H.; Matsumoto, N.; Kojima, M.; Dahan, F.; Tuchagues, J.-P.; Re, N.; Iijima, S. *Chem.−Eur. J.* **2006**, *12*, 4536−4549. (b) Sunatsuki, Y.; Ikuta, Y.; Matsumoto, N.; Ohta, H.; Kojima, M.; Iijima, S.; Hayami, S.; Maeda, Y.; Kaizaki, S.; Dahan, F.; Tuchagues, J.-P. *Angew. Chem., Int. Ed.* **2003**, *42*, 1614−1618. (c) Ikuta, Y.; Ooidemizu, M.; Yamahata, Y.; Yamada, M.; Osa, S.; Matsumoto, N.; Iijima, S.; Sunatsuki, Y.; Kojima, M.; Dahan, F.; Tuchagues, J.-P. *Inorg. Chem.* **2003**, *42*, 7001−7017. (d) Yamada, M.; Ooidemizu, M.; Ikuta, Y.; Osa, S.; Matsumoto, N.; Iijima, S.; Kojima, M.; Dahan, F.; Tuchagues, J.-P. *Inorg. Chem.* **2003**, *42*, 8406−8416. (e) Sunatsuki, Y.; Ohta, H.; Kojima, M.; Ikuta, Y.; Goto, Y.; Matsumoto, N.; Iijima, S.; Akashi, H.; Kaizaki, S.; Dahan, F.; Tuchagues, J.-P. *Inorg. Chem.* **2004**, *43*, 4154−4171. (f) Yamada, M.; Fukumoto, E.; Ooidemizu, M.; Bréfuel, N.; Matsumoto, N.; Iijima, S.; Kojima, M.; Re, N.; Dahan, F.; Tuchagues, J.-P. *Inorg. Chem.* **2005**, *44*, 6967−6974. (g) Bréfuel, N.; Imatomi, S.; Torigoe, H.; Hagiwara, H.; Shova, S.; Meunier, J. -F.; Bonhommeau, S.; Tuchagues, J. -P.; Matsumoto, N. *Inorg. Chem.* **2006**, *45*, 8126−8135.

(7) Arata, S.; Torigoe, H.; Iihoshi, T.; Matsumoto, N.; Dahan, F.; Tuchagues, J.-P. *Inorg. Chem.* **2005**, *44*, 9288−9292.

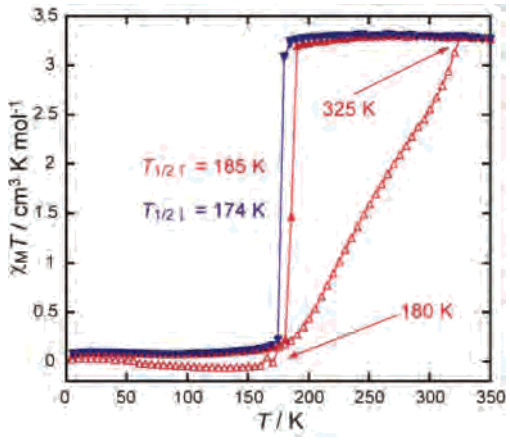

Figure 1. Magnetic behavior of $[Fe^{II}(HL^{H,Me})_2](ClO_4)_2 \cdot 1.5MeCN$ (**1**) in the form of $\chi_M T$ versus T plots. The sample was warmed from 5 to 350 K (△) and then cooled from 350 to 5 K (▽) in the first cycle, and then the sample was warmed from 5 to 350 K (▲) and then cooled from 350 to 5 K (▼) in the second cycle at a sweep rate of 1 K min^{-1}.

molecule (5.8% weight loss) after 7.5 h, and a temperature slightly higher than room temperature is needed to remove the remaining MeCN molecules (ca. 0.5MeCN). There are many examples in which the crystal solvents are strongly trapped in the crystal cavity and the elimination temperature is much higher than the boiling point.[8] The present solvated **1** is not such a case.

Magnetic Properties of $[Fe^{II}(HL^{H,Me})_2](ClO_4)_2 \cdot 1.5MeCN$ (1). Magnetic susceptibilities were measured in the 5−350 K range at a sweep rate of 1 K min^{-1} in an applied magnetic field of 0.5 T. Freshly prepared crystals were promptly ground, and the SQUID sample was quickly prepared, and then the sample was set in the SQUID device. The sample was quickly cooled from room temperature to 5 K within a few seconds, and the magnetic susceptibility was measured in the warming mode from 5 to 350 K as the first run and then measured in the cooling mode from 350 to 5 K as the second run (first cycle). Following the first cycle, magnetic susceptibilities were measured in the warming mode from 5 to 350 K as the third run and then measured in the cooling mode from 350 to 5 K as the fourth run (second cycle).

The $\chi_M T$ versus T plots are shown in Figure 1. In the first cycle, the magnetic behavior is different in the warming mode than it is in the cooling mode. Upon increasing the temperature from 5 K in the first run, the initial $\chi_M T$ value of 0.03 cm^3 K mol^{-1}, which is the expected value for LS Fe^{II} ($S = 0$), is nearly constant in the temperature range of 5−180 K. Upon increasing the temperature beyond 180 K, the $\chi_M T$ value gradually increases to approach a plateau value of about 3.3 cm^3 K mol^{-1} between 325 and 350 K, demonstrating the gradual spin transition from the LS to HS Fe^{II} state. The $\chi_M T$ value of about 3.3 cm^3 K mol^{-1} is the expected value for HS Fe^{II} ($S = 2$). We note that acetonitrile molecules as the crystal solvent are removed during the warming mode of this first run and that the sample at 350 K at the end of the first run should be the desolvated sample on the basis of the TGA results. Upon lowering the temperature from 350 to 5 K in the second run, the $\chi_M T$ value of about 3.3 cm^3 K mol^{-1} is constant in the region of 350−185 K, and the value steeply decreases at around 180 K from about 3.1 cm^3 K mol^{-1} to nearly zero. The evaluated $T_{1/2\downarrow}$ value is 174 K.

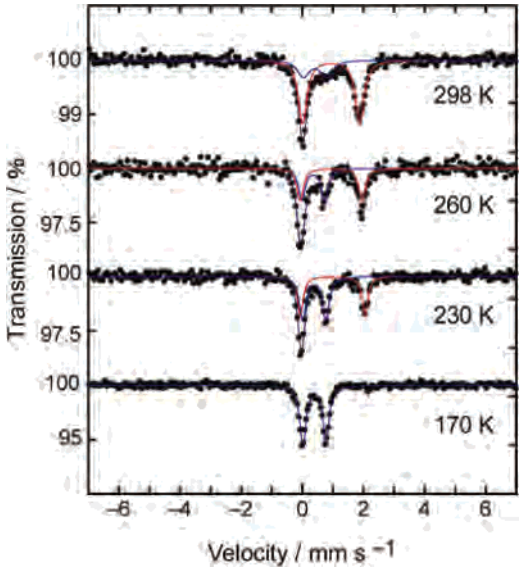

Figure 2. Selected ^{57}Fe Mössbauer spectra of $[Fe^{II}(HL^{H,Me})_2](ClO_4)_2 \cdot 1.5MeCN$ (**1**) recorded at 298, 260, 230, and 170 K upon warming the sample from 78 K.

In the second cycle, the magnetic behavior is similar in the warming and cooling modes, except in the transition temperature. Upon increasing the temperature from 5 to 350 K in the third run, the $\chi_M T$ value of about 0.1 cm^3 K mol^{-1} is constant in the region of 5−170 K, and the value steeply increases at around 180 K from about 0.2 to 3.3 cm^3 K mol^{-1}. Upon lowering the temperature from 350 to 5 K in the fourth run, the behavior of the $\chi_M T$ value perfectly agrees with the second run of the first cycle. As shown in Figure 1, the critical temperatures for the warming ($T_{1/2\uparrow}$) and cooling ($T_{1/2\downarrow}$) modes (185 and 174 K, respectively) indicate the occurrence of ca. 11 K wide thermal hysteresis. The difference in magnetic behavior between the first and third runs may be ascribed to the removal of 1.5MeCN molecules from the TGA results.

Mössbauer Spectra of $[Fe^{II}(HL^{H,Me})_2](ClO_4)_2 \cdot 1.5MeCN$ (1). Selected Mössbauer spectra in the warming mode are shown in Figure 2. Table 1 lists the Mössbauer parameters at each selected temperature in the warming and cooling modes. The Mössbauer spectra in the warming and cooling modes are nearly the same. In the temperature region of 78−170 K, each spectrum consists only of a doublet attributable to the LS Fe^{II} species (e.g., at 78 K, isomer shift $\delta = 0.42$ mm s^{-1}, quadrupole splitting $\Delta E_Q = 0.73$ mm s^{-1}). Upon increasing the sample temperature from 170 to 298 K, the relative intensity of the doublet due to the LS Fe^{II} species decreases, whereas that of the doublet due to the HS Fe^{II} species increases, showing a gradual one-step SC behavior.

A deconvolution analysis of the spectra was performed to determine the HS versus total Fe^{II} molar fraction, n_{HS}. The plots of the variation of n_{HS} with temperature derived from the Mössbauer spectra are shown in Figure 3, together with

(8) Amoore, J. J. M.; Kepert, C. J.; Cashion, J. D.; Moubaraki, B.; Neville, S. M.; Murray, K. S. *Chem.—Eur. J.* **2006**, *12*, 8220−8227.

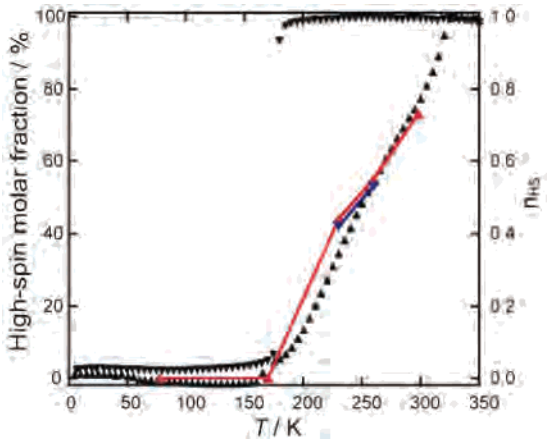

Figure 3. Molar fraction of HS versus total Fe^{II}, n_{HS}, for $[Fe^{II}(HL^{H,Me})_2](ClO_4)_2$·1.5MeCN (**1**) in the warming (▲) and cooling modes (▼) obtained by deconvolution analysis of the Mössbauer spectra, together with n_{HS} values obtained from the magnetic susceptibility measurements. n_{HS} was calculated by using the equation $(\chi_M T)_{obs} = n_{HS}(\chi_M T)_{HS} + (1 - n_{HS})(\chi_M T)_{LS}$, with $(\chi_M T)_{HS} = 3.5$ cm^3 K mol^{-1} and $(\chi_M T)_{LS} = 0.0$ cm^3 K mol^{-1} as limiting values.

Table 1. Mössbauer Parameters for $[Fe^{II}(HL^{H,Me})_2](ClO_4)_2$·1.5MeCN (**1**)

T (K)	δ^a (mm s^{-1})	ΔE_Q (mm s^{-1})	Γ^b (mm s^{-1})	area ratio (%)
A. On Heating after Rapid Cooling-Down to 78 K				
298	0.94	1.87	0.33	73
	0.41	0.76	0.47	27
260	0.94	2.02	0.26	55
	0.37	0.72	0.34	45
230	0.99	2.11	0.22	44
	0.39	0.76	0.25	56
170	0.40	0.76	0.24	100
78	0.42	0.73	0.25	100
B. On Slow Cooling from Room Temperature				
260	0.95	2.00	0.27	53
	0.35	0.72	0.34	47
230	1.01	2.13	0.24	42
	0.39	0.76	0.27	58

[a] Isomer shift data are reported with respect to iron foil. [b] Full width at half height.

the variation of n_{HS} derived from the magnetic susceptibility measurements. The plots in the warming and cooling modes are nearly the same. As is clearly apparent from Figure 3 and Table 1, the Mössbauer and magnetic susceptibility results are not consistent in the cooling mode. This inconsistency is due to the nonremoval of MeCN molecules because of the sealing up of the cell when making the Mössbauer measurement.

Description of the Structure of $[Fe^{II}(HL^{H,Me})_2](ClO_4)_2$·1.5MeCN (1). The X-ray diffraction data were collected at 296 K (intermediate between HS and LS states) and 150 K (LS state). The crystal structure in the HS form could not be determined because the LS → HS transition accompanies the desolvation of acetonitrile, which induces cracks in the crystal. The crystallographic data at 296 and 150 K are given in Table 2. The unit cell parameters at 296 K are similar to those at 150 K, and the monoclinic space group $C2/c$ ($Z = 4$) is retained in both states. The structure consists of a $[Fe^{II}(HL^{H,Me})_2]^{2+}$ cation, two ClO_4^- anions, and MeCN molecules.

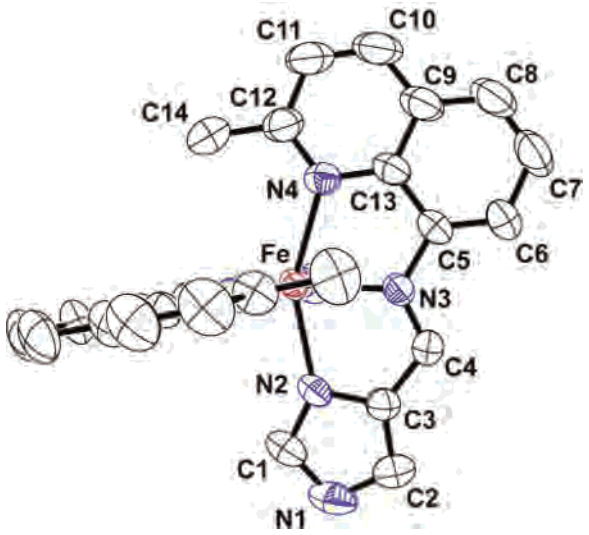

Figure 4. Molecular structure of $[Fe^{II}(HL^{H,Me})_2](ClO_4)_2$·1.5MeCN (**1**) at 296 K with numbered atoms. H atoms, ClO_4^- ions, and the MeCN molecule are omitted for clarity.

Table 2. Crystallographic Data for $[Fe^{II}(HL^{H,Me})_2](ClO_4)_2$·1.5MeCN (**1**)

params	296 K	150 K
formula	$C_{31}H_{28.5}N_{9.5}FeCl_2O_8$	$C_{31}H_{28.5}N_{9.5}FeCl_2O_8$
fw	788.88	788.88
cryst syst	monoclinic	monoclinic
No.	$C2/c$ (No. 15)	$C2/c$ (No. 15)
a (Å)	19.733(8)	19.563(7)
b (Å)	12.901(5)	12.713(5)
c (Å)	17.025(6)	16.837(8)
β (deg)	121.261(15)	121.099(15)
V (Å^3)	3704.9(24)	3585.6(26)
Z	4	4
F(000)	1620	1620
λ (Å)	0.71075	0.71075
T (K)	296 ± 2	150 ± 2
D_{calcd} (g cm^{-3})	1.414	1.461
μ(Mo Kα) (cm^{-1})	6.111	6.315
θ range (deg min-max)	3.2−27.5	3.2−27.5
no. of data collected	17 678	16 670
no. of unique data	4225	4091
R (int)	0.062	0.052
no. of variable params	231	240
no. of obsd reflns[a]	2565	2491
R^b	0.0759	0.0762
$w_R{}^c$	0.1677	0.1749
S	1.008	1.003
(Δ/ρ)max, min, (eÅ^{-3})	0.81, −0.61	1.33, −0.54

[a] Data with $F_o > 4\sigma(F)$. [b] $R = \Sigma||F_o| - |F_c||/\Sigma|F_o|$. [c] $wR = [\Sigma w(|F_o^2| - |F_c^2|)^2/\Sigma w|F_o^2|^2]^{1/2}$.

Structure at 296 K. The molecular structure in a numbered atom scheme at 296 K is shown in Figure 4, and selected bond lengths and angles are given in Table 3. The Fe^{II} ion assumes an octahedral coordination environment made up of six N donor atoms of two tridentate $HL^{H,Me}$ ligands. The iron atom lies on a 2-fold rotational axis, and this defines the crystallographically unique unit as half of the $[Fe^{II}(HL^{H,Me})_2]^{2+}$ cation. At 296 K, the Fe−N bond lengths (2.095(2)−2.187(2) Å) are slightly shorter than the values expected for an HS Fe^{II} complex with six similar N donor atoms[7] and longer than those for an LS complex. This result agrees with the Mössbauer and magnetic susceptibility results.

Table 3. Relevant Coordination Bond Lengths (Angstroms) and Angles (deg) for $[Fe^{II}(HL^{H,Me})_2](ClO_4)_2$ 1.5MeCN (**1**) at 296 and 150 K

params	296 K	150 K
Fe−N(2)	2.152(3)	1.966(3)
Fe−N(3)	2.095(2)	1.938(2)
Fe−N(4)	2.187(2)	2.037(2)
Fe−N(2)*[a]	2.152(3)	1.966(3)
Fe−N(3)*	2.095(2)	1.938(2)
Fe−N(4)*	2.187(2)	2.037(2)
N(2)−Fe−N(2)*	88.89(11)	89.88(12)
N(2)−Fe−N(3)	76.26(9)	80.31(10)
N(2)−Fe−N(3)*	92.40(10)	90.86(11)
N(2)−Fe−N(4)	152.83(9)	161.75(9)
N(2)−Fe−N(4)*	92.26(10)	90.48(11)
N(2)*−Fe−N(3)	92.40(10)	90.86(11)
N(2)*−Fe−N(3)*	76.26(9)	80.31(10)
N(2)*−Fe−N(4)	92.26(10)	90.48(11)
N(2)*−Fe−N(4)*	152.83(9)	161.75(9)
N(3)−Fe−N(3)*	164.25(9)	167.56(11)
N(3)−Fe−N(4)	76.57(10)	81.44(11)
N(3)−Fe−N(4)*	114.24(11)	107.18(11)
N(3)*−Fe−N(4)	114.24(11)	107.18(11)
N(3)*−Fe−N(4)*	76.57(10)	81.44(11)
N(4)−Fe−N(4)*	98.82(10)	94.81(11)

[a] Symmetry operations: (*), $-x+1, y, -z+{}^3/_2$.

Intermolecular interactions and the extended network structure at 296 K are shown in Figures 5 and 6a,b, respectively. As shown in Figures 5 and 6a, the perchlorate ions play the role of connector through bifurcated hydrogen bonds between O^- and the imidazole NH groups of two neighboring $[Fe^{II}(HL^{H,Me})_2]^{2+}$ cations. Two ClO_4^- ions are hydrogen bonded to the imidazole NH groups of two neighboring $[Fe^{II}(HL^{H,Me})_2]^{2+}$ cations, and two adjacent cations form $\pi-\pi$ stacking in the $HL^{H,Me}$ ligands between the two quinolyl rings, which produce a 2D extended structure. Hydrogen bond lengths and intermolecular C···C contacts are O(1)···N(1) = 2.892(6), O(1)···N(1)** = 3.053(4), N(1)**···O(1)** = 2.892(6), N(1)···O(1)** = 3.053(4), C(10)···C(12)*** = 3.571(7), and C(12)···C(10)*** = 3.571(7) Å at 296 K, as shown in Table 4. Hydrogen bond lengths are shorter than those of other complexes having bifurcated hydrogen bond networks,[9a] and intermolecular C···C contacts are fewer and longer than those of other SC complexes.[5a−e] It should be noted that both of the imidazole NH groups and the quinolyl rings of the $[Fe^{II}(HL^{H,Me})_2]^{2+}$ cation participate in the construction of the 2D extended structure. As shown in Figure 6b, each 2D layer assumes a thickness corresponding to the molecular size of one complex, and the 2D layer is parallel to the *bc* plane and accumulates in the *a* direction. In the *a* direction, the 2D layers are mainly connected by weaker van der Waals interactions.

One MeCN molecule lies on a 2-fold rotational axis and exists as an isolated crystal solvent in a cavity of the 2D layer (Figure 6a). The large thermal parameters indicate that the molecule does not interact with the rest of the molecule and is easily removed. Acetonitrile (0.5MeCN) could not be found, probably as a result of the removal of MeCN at 296 K, as suggested by the TGA analysis.

Structure at 150 K. The complex assumes an octahedral coordination environment similar to that of the complex at 296 K. At 150 K, the Fe−N bond lengths (1.938(2)−2.037(2) Å) are typical for the LS Fe^{II} complex.[7] The average Fe−N bond length decreases by 0.165 Å from 2.145 Å at 296 K to 1.980 Å at 150 K. The N−Fe−N bond angles shift toward the value for a regular octahedron at 150 K.

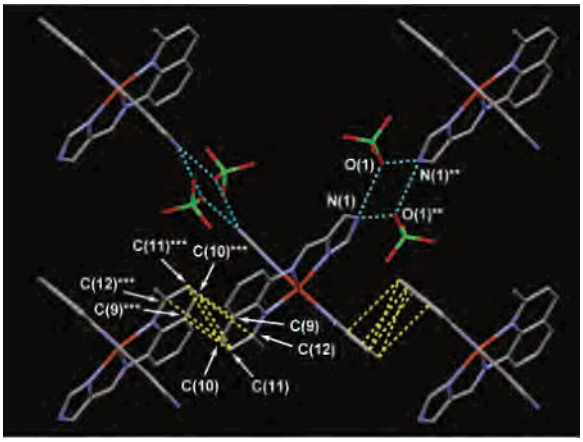

Figure 5. Intermolecular interactions of $[Fe^{II}(HL^{H,Me})_2](ClO_4)_2$·1.5MeCN (**1**) at 296 K. Two ClO_4^- ions are bifurcated and hydrogen bonded to the imidazole NH groups of two neighboring $[Fe^{II}(HL^{H,Me})_2]^{2+}$ cations, and two adjacent cations form $\pi-\pi$ stacking in the $HL^{H,Me}$ ligands between the two quinolyl rings. The symbols ** and *** denote the symmetry operations of $(-x+1, -y+1, -z+2)$ and $(-x+1, -y, -z+1)$, respectively.

Table 4. Hydrogen Bond Lengths (Angstroms) and Intermolecular C···C Contacts (Angstroms) Shorter Than the van der Waals Distance (3.6 Å) for $[Fe^{II}(HL^{H,Me})_2](ClO_4)_2$·1.5MeCN (**1**) at 296 and 150 K

	296 K	150 K
Hydrogen Bonds		
O(1)···N(1)	2.892(6)	2.918(4)
O(1)···N(1)**[a]	3.053(4)	2.853(4)
N(1)**···O(1)**	2.892(6)	2.918(4)
N(1)···O(1)**	3.053(4)	2.853(4)
Intermolecular C···C Contacts		
C(9)···C(11)***		3.514(6)
C(10)···C(11)***		3.515(5)
C(10)···C(12)***	3.571(7)	3.542(5)
C(11)···C(9)***		3.514(6)
C(11)···C(10)***		3.515(5)
C(12)···C(10)***	3.571(7)	3.542(5)

[a] Symmetry operations: (**), $-x+1, -y+1, -z+2$; (***), $-x+1, -y, -z+1$.

The extended network structure is similar to that of the complex at 296 K. The lengths of the intermolecular interactions are slightly different. Hydrogen bond lengths and intermolecular C···C contacts are O(1)···N(1) = 2.918(4), O(1)···N(1)** = 2.853(4), N(1)**···O(1)** = 2.918(4), N(1)···O(1)** = 2.853(4), C(9)···C(11)*** = 3.514(6), C(10)···C(11)*** = 3.515(5), C(10)···C(12)*** = 3.542(5), C(11)···C(9)*** = 3.514(6), C(11)···C(10)*** = 3.515(5), and C(12)···C(10)*** = 3.542(5) Å at 150 K (Table 4). Hydrogen bond lengths are shorter than those at 296 K, and there are more intermolecular C···C contacts, which are shorter than those at 296 K. These results show that both hydrogen bonds and $\pi-\pi$ interactions are more effective than those at 296 K.

One MeCN molecule lies on a 2-fold rotational axis and exists as an isolated crystal solvent in a cavity of the 2D layer. Acetonitrile (0.5MeCN) could not be found, although

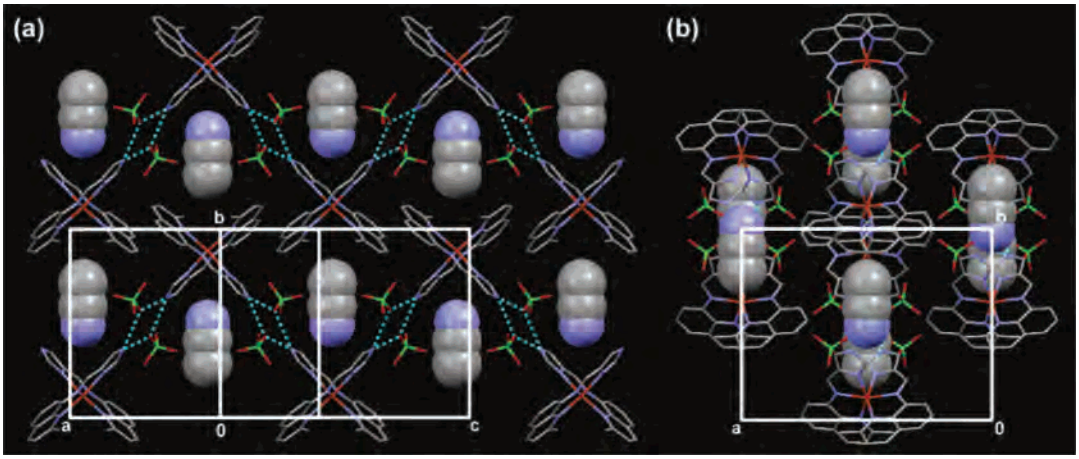

Figure 6. (a) Top view of a 2D extended structure of $[Fe^{II}(HL^{H,Me})_2](ClO_4)_2 \cdot 1.5MeCN$ (**1**) at 296 K. The 2D network is formed by bifurcated hydrogen bonds and $\pi-\pi$ interactions, whereas the one MeCN molecule exists as an isolated crystal solvent in a cavity of the 2D layer. The 2D layer is parallel to the *bc* plane. (b) Side view showing the stacking of the 2D extended structures. Each 2D layer assumes a thickness corresponding to the molecular size of one complex and accumulates in the *a* direction.

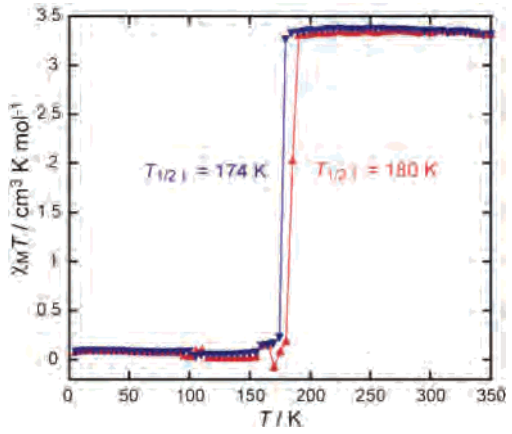

Figure 7. Magnetic behavior of $[Fe^{II}(HL^{H,Me})_2](ClO_4)_2$ (**1′**) in the form of $\chi_M T$ versus T plots. The sample was quickly cooled from room temperature to 5 K, and $\chi_M T$ values were first measured in the course of warming from 5 to 350 K at a sweep rate of 1 K min^{-1} (▲). $\chi_M T$ values were then measured in the course of cooling from 350 to 5 K at a sweep rate of 1 K min^{-1} (▼).

a few residual peaks attributable to it were located between 2D layers, suggesting that 0.5MeCN exists there.

Magnetic Properties of Desolvated Sample $[Fe^{II}(HL^{H,Me})_2](ClO_4)_2$ (1′). To examine the effect of solvent molecules on the SC behavior, desolvated sample **1′** was prepared by heating **1** to 100 °C for 5 h. The formula of $[Fe^{II}(HL^{H,Me})_2](ClO_4)_2$ (**1′**) was confirmed by elemental analysis.

The $\chi_M T$ versus T plots are shown in Figure 7. As shown in Figure 7, the desolvated sample showed a steep SC behavior with hysteresis, and the critical temperatures for the warming ($T_{1/2\uparrow}$) and cooling ($T_{1/2\downarrow}$) modes (180 and 174 K, respectively) indicate the occurrence of ca. 6 K wide thermal hysteresis. These results suggest that the abrupt spin transition with the hysteresis of **1** in the second cycle is directly related to the removal of solvent molecules.

Mössbauer Spectra of Desolvated Sample $[Fe^{II}(HL^{H,Me})_2](ClO_4)_2$ (1′). Representative Mössbauer spectra are shown in Figure 8. Upon increasing the temperature of the sample after rapid cooling to 78 K, spectra were recorded at 78, 170, 175, 180, 190, 200, and 298 K. In the range of 78−

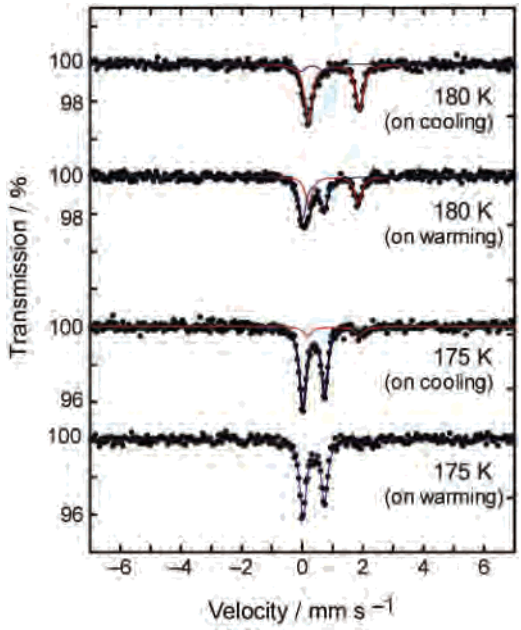

Figure 8. Selected ^{57}Fe Mössbauer spectra of $[Fe^{II}(HL^{H,Me})_2](ClO_4)_2$ (**1′**) recorded at 180 and 175 K upon warming the sample after rapid cooling to 78 K and upon gradual cooling from 300 K.

175 K, each spectrum consists only of a doublet attributable to the LS Fe^{II} species (e.g., at 78 K, $\delta = 0.40$ mm s^{-1}, $\Delta E_Q = 0.72$ mm s^{-1}). Upon increasing the temperature above 175 K, the relative intensity of the doublet due to the LS state decreases, whereas that of the doublet due to the HS state increases, showing a steep one-step SC behavior. Above 190 K, only the doublet due to the HS species is observed. During slow cooling of the sample from 298 to 78 K, Mössbauer spectra were recorded at 190, 180, 175, and 170 K. At 190 K, the spectrum consists only of a doublet attributable to the HS Fe^{II} species ($\delta = 1.02$ mm s^{-1}, $\Delta E_Q = 1.64$ mm s^{-1}). Upon lowering the temperature below 190 K, the relative intensity of the doublet due to the HS state decreases, whereas that of the doublet due to the LS state increases.

A deconvolution analysis of the spectra was performed to determine the HS versus total Fe^{II} molar fraction, n_{HS}, and the results are presented in Figure 9 and Table 5. As is clearly

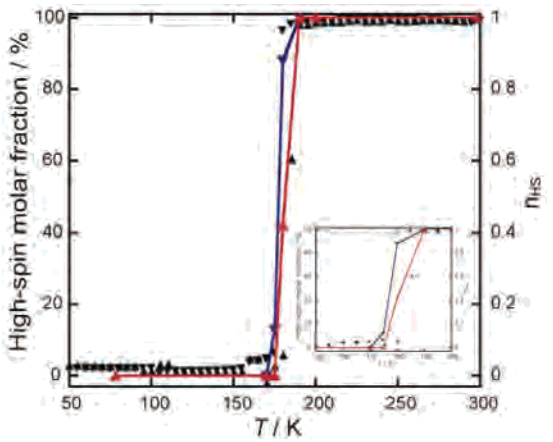

Figure 9. Molar fraction of HS versus total Fe^{II}, n_{HS}, for $[Fe^{II}(HL^{H,Me})_2](ClO_4)_2$ (**1′**) in the warming (▲) and cooling modes (▼) obtained by deconvolution analysis of the Mössbauer spectra, together with n_{HS} obtained from the magnetic susceptibility measurements. n_{HS} was calculated by using the equation $(\chi_M T)_{obs} = n_{HS}(\chi_M T)_{HS} + (1 - n_{HS})(\chi_M T)_{LS}$, with $(\chi_M T)_{HS} = 3.5$ cm^3 K mol^{-1} and $(\chi_M T)_{LS} = 0.0$ cm^3 K mol^{-1} as limiting values. The inset reveals hysteresis.

Table 5. Mössbauer Parameters for $[Fe^{II}(HL^{H,Me})_2](ClO_4)_2$ (**1′**)

T (K)	δ^a (mm s^{-1})	ΔE_Q (mm s^{-1})	Γ^b (mm s^{-1})	area ratio (%)
A. On Heating after Rapid Cooling to 78 K				
298	0.94	1.10	0.26	100
200	1.03	1.58	0.30	100
190	1.01	1.63	0.31	100
180	1.03	1.65	0.28	42
	0.37	0.71	0.29	58
175	0.38	0.71	0.25	100
170	0.37	0.70	0.27	100
78	0.40	0.72	0.25	100
B. On Slow Cooling from Room Temperature				
190	1.02	1.64	0.30	100
180	1.05	1.67	0.29	88
	0.35	0.73	0.28	12
175	1.03	1.71	0.29	13
	0.38	0.73	0.25	87
170	0.39	0.72	0.26	100

[a] Isomer shift data are reported with respect to iron foil. [b] Full width at half height.

apparent from Figure 9 and Table 5, the Mössbauer and magnetic susceptibility results are almost consistent, and hysteresis is also observed in the Mössbauer measurements.

Discussion

In this study, a 2D iron(II) SC complex, $[Fe^{II}(HL^{H,Me})_2](ClO_4)_2$·1.5MeCN (**1**), with the coexistence of bifurcated hydrogen bonds and $\pi-\pi$ interactions was synthesized and characterized. This complex showed a spin transition with wide hysteresis, and the solvent molecules significantly changed the SC behavior. The 2D extended network structure is constructed of bifurcated hydrogen bonds and $\pi-\pi$ interactions in which bifurcated hydrogen bonds produce 1D zigzag networks and $\pi-\pi$ interactions also produce 1D networks. As this occurs, the 2D network is formed.

We note that **1** has bifurcated hydrogen bonds.[9] Linear hydrogen bonds between −OH or −NH groups and proton acceptors with highly electronegative atoms are one of the most important types of interactions in the modern chemistry of material design. Bifurcated hydrogen bonds also play important roles in supramolecular chemistry, aiding in self assembly[9b] and chiral recognition.[9c] Rozas et al. investigated the nature of bifurcated hydrogen bonds and showed that they are energetically weaker interactions than regular hydrogen bonds.[9d] The investigation of crystal databases revealed that there are bifurcated hydrogen bonds in a number of crystal structures.[9a,e−g] There are a few examples that show that bifurcated hydrogen bonds construct the cooperative network in an SC complex.[9g]

Although the MeCN molecule as the crystal solvent shows no intermolecular interaction with the rest of the molecule, exists only in a cavity of the 2D network, and is easily removed, the solvent significantly affected the SC behavior. The consideration of "why do the MeCN molecules affect the SC behavior?" can give an idea of "what are the important factors to induce spontaneous spin transition from one SC site all over other SC sites?" In addition to a network structure that makes possible a spin transition over all SC sites, it is also necessary to have structural flexibility or fitness to make a large structural change in the crystal lattice possible before and after a spin transition. Recently, we have reported a series of SC complexes $[Fe^{II}(H_3L^{Me})]Cl\cdot X$ (H_3L^{Me} = tris[2-{[(2-methylimidazol-4-yl)methylidene]amino}ethyl]-amine, X = PF_6, AsF_6, SbF_6, CF_3SO_3).[6a] This series of SC complexes crystallized in the same crystal system and space group with similar cell dimensions. The crystal structure is a 2D network structure constructed of NH···Cl^- hydrogen bonds, whereas the anion X exists as an isolated anion and occupies the space between the 2D sheets. The only difference among the complexes is the volume occupied by the counteranion. The SC behavior depends on the counteranion. The SC can exhibit a one-step HS ↔ (HS + LS)/2 (X = PF_6^-), a two step HS ↔ (HS + LS)/2 ↔ LS (X = AsF_6^-), a gradual one-step HS ↔ LS (X = SbF_6^-), and a steep one-step with hysteresis HS ↔ LS (X = $CF_3SO_3^-$). The various observed SC behaviors are primarily correlated to the relative volume of the counteranion. This example demonstrates that the occupied space of the counteranion, not including chemical bonds to the rest of the structure, is sufficient to produce SC properties such as steepness, multistep, and hysteresis. This means that the occupied volume of the counteranion effectively induces SC properties with steepness and hysteresis. There are many reports similar to this idea.[5] The present result gives one experimental result to approach a better understanding of SC behavior.

Experimental Section

General and Materials. All of the chemicals and solvents, obtained from Tokyo Kasei Co., Ltd., and Wako Pure Chemical Industries, Ltd., were of reagent grade and were used for the

(9) (a) Fourmigué, M.; Mézière, C.; Dolou, S. *Cryst. Growth Des.* **2003**, *3*, 805−810. (b) Conn, M. M.; Rebek, J. *Chem. Rev.* **1997**, *97*, 1647−1668. (c) Kim, S.-G.; Kim, K.-H.; K, Y. K.; Shin, S. K.; Ahn, K. H. *J. Am. Chem. Soc.* **2003**, *125*, 13819−13824. (d) Rozas, I.; Alcorta, I.; Elguero, J. *J. Phys. Chem. A* **1998**, *102*, 9925−9932. (e) Sakagami-Yoshida, N.; Teramoto, M.; Hioki, A.; Fuyuhiro, A.; Kaizaki, S. *Inorg. Chem.* **2000**, *39*, 5717−5724. (f) Ni-iya, K.; Fuyuhiro, A.; Yagi, T.; Nasu, S.; Kuzushita, K.; Morimoto, S.; Kaizaki, S. *Bull. Chem. Soc. Jpn.* **2001**, *74*, 1891−1897. (g) Leita, B. A.; Moubaraki, B.; Murray, K. S.; Smith, J. P. *Polyhedron* **2005**, *24*, 2165−2172.

syntheses without further purification. All of the synthetic procedures were carried out in air.

$[Fe^{II}(HL^{H,Me})_2](ClO_4)_2 \cdot 1.5MeCN$ (1). A solution of 8-amino-2-methylquinoline (1.585 g, 10 mmol) in 5 mL of methanol was added to a solution of 4-formylimidazole (0.965 g, 10 mmol) in 15 mL of methanol. The resulting solution was stirred on a hot plate at 40 °C for 3 h. The ligand solution was used for the synthesis of the Fe^{II} complex without isolating the ligand. A solution of $Fe^{II}(ClO_4)_2 \cdot 6H_2O$ (1.818 g, 5 mmol) in 5 mL of methanol was added to the ligand solution (10 mmol). The resulting solution was stirred for 30 min and then filtered. The filtrate was allowed to stand for several days, during which time the precipitated black powder was collected by suction filtration, washed with a small volume of methanol, and dried in vacuo. Recrystallization was performed from the acetonitrile solution. Black crystals were collected by suction filtration. Yield: 2.117 g (54%). Anal. Calcd for $[Fe^{II}(HL^{H,Me})_2](ClO_4)_2 \cdot 1.5MeCN$: C, 47.20; H, 3.64; N, 16.87. Found: C, 47.13; H, 3.77; N, 16.93. IR (KBr): $\nu_{C=N}$ 1609 cm^{-1}, $\nu_{Cl-O}(ClO_4^-)$ 1086 cm^{-1}.

$[Fe^{II}(HL^{H,Me})_2](ClO_4)_2$ (1′). Desolvated sample **1′** was prepared by heating **1** to 100 °C using a Sibata GTO-350D glass tube oven for 5 h. Weight loss corresponding to 1.5MeCN per metal complex was observed. Anal. Calcd for $[Fe^{II}(HL^{H,Me})_2](ClO_4)_2$: C, 46.24; H, 3.33; N, 15.41. Found: C, 46.46; H, 3.44; N, 15.39. IR (KBr): $\nu_{C=N}$ 1611 cm^{-1}, $\nu_{Cl-O}(ClO_4^-)$ 1093 cm^{-1}.

Caution. Perchlorate salts of metal complexes with organic ligands are potentially explosive. Only small quantities of the compound should be prepared, and they should be handled with much care. The TGA measurement and the desolvation process were carried out using a small quantity of the samples (ca. 10−20 mg), and the highest temperature was 100 °C.

Physical Measurements. C, H, and N elemental analyses were performed by Kikue Nishiyama at the Center for Instrumental Analysis of Kumamoto University. Infrared spectra were recorded at room temperature using a Nicolet Avatar 370 DTGS (Thermo Electron Corporation) spectrometer with samples in KBr disks. Magnetic susceptibilities were measured in the 5−350 K temperature range at a sweep rate of 1 K min^{-1} under an applied magnetic field of 0.5 T using an MPMS5 SQUID susceptometer (Quantum Design). The apparatus was calibrated with palladium metal. Corrections for diamagnetism were applied by using Pascal's constants.[10] Mössbauer spectra were recorded using a Wissel 1200 spectrometer and a proportional counter. $^{57}Co(Rh)$ moving in a constant acceleration mode was used as the radioactive source. Hyperfine parameters were obtained by a least-squares fitting of the Lorentzian peaks. Isomer shifts were reported relative to iron foil at 293 K. The sample temperature was controlled by means of a Heli-tran liquid-transfer refrigerator (Air Products and Chemicals, Inc.) to within an accuracy of ±0.5 K. Thermogravimetric data for **1** was collected on a TG/DTA6200 (SII Nano Technology Inc.) instrument under an air atmosphere.

Crystallographic Data Collection and Structure Determination for $[Fe^{II}(HL^{H,Me})_2](ClO_4)_2 \cdot 1.5MeCN$ (1) at 296 and 150 K. A black block crystal having approximate dimensions of 0.51 × 0.34 × 0.34 mm^3 was mounted on a glass fiber. All measurements were made on a Rigaku RAXIS RAPID imaging plate area detector with graphite monochromated Mo Kα radiation (λ = 0.71075 Å). The temperature of the crystal was maintained at the selected value by means of a Rigaku cooling device to within an accuracy of ±2 K. The data were corrected at 296 K to a maximum 2θ value of 54.9°. Following the measurement at 296 K, the crystal was then rapidly cooled to 150 K with a Rigaku cooling device, but it lost crystallinity by the end of the cooling process. A new black block crystal having approximate dimensions of 0.38 × 0.17 × 0.16 mm^3 was then mounted on a Rigaku RAXIS RAPID imaging plate area detector with graphite monochromated Mo Kα radiation (λ = 0.71075 Å). The data were corrected at 150 K to a maximum 2θ value of 55.0°. There were 2565 reflections collected at 296 K, of which 575 were unique (R_{int} = 0.062), and 2491 reflections collected at 150 K, of which 553 were unique (R_{int} = 0.052); equivalent reflections were merged. Empirical absorption corrections were applied for $T_{min-max}$ = 0.538−0.815 at 296 K and $T_{min-max}$ = 0.513−0.903 at 150 K. The data were corrected for Lorentz and polarization effects.

The structures were solved by direct methods[11] and expanded using the Fourier technique.[12] At 296 K, the structures were refined on F^2 full-matrix least squares with anisotropic displacement parameters for all non-hydrogen atoms except atoms of one MeCN molecule. One MeCN molecule located in a cavity of the 2D layer was found, and its non-hydrogen atoms were refined isotropically, whereas 0.5MeCN could not be found. This inconsistency can be due to the easy removal of the MeCN molecule at ambient temperature, suggested by the TGA results. At 150 K, the structures were refined on F^2 full-matrix least squares with anisotropic displacement parameters for all non-hydrogen atoms except for 0.5MeCN. One MeCN molecule located in a cavity of the 2D layer was found, and its non-hydrogen atoms were refined anisotropically. A few residual peaks were located between 2D layers, suggesting that 0.5MeCN exists there. However, because of the low values of the corresponding electron densities, it was not enough to model that structure. Hydrogen atoms were fixed in calculated positions and refined by using a riding model, with the exception of those bonded to C(16), which had a symmetrical problem. The maximum and minimum peaks on the final-difference Fourier map were 0.81 and −0.61 $eÅ^{-3}$ at 296 K and 1.33 and −0.54 $eÅ^{-3}$ at 150 K. The atomic scattering factors and anomalous dispersion terms were taken from the standard compilation.[13] All of the calculations were performed by using the Crystal Structure crystallographic software package.[14,15] The crystal data collection and refinement parameters are given in Table 2.

Acknowledgment. This work was supported in part by a Grant-in-Aid for Science Research (no. 16205010) from the Ministry of Education, Science, Sports, and Culture, Japan.

Supporting Information Available: X-ray crystallographic files for **1**. See http://www.rcs.org/suppdata/dt/ for other crystallographic data. This material is available free of charge via the Internet at http://pubs.acs.org.

IC061960A

(10) Kahn, O. *Molecular Magnetism;* VCH: Weinheim, Germany, 1993.

(11) Altomare, A.; Cascarano, G.; Giacovazzo, C.; Guagliardi, A.; Burla, M.; Polidori, G.; Camalli, M. *J. Appl. Cryst.* **1994**, *27*, 435.

(12) Beurskens, P. T.; Admiraal, G.; Beurskens, G.; Bosman, W. P.; de Gelder, R.; Israel, R.; Smits, J. M. M. *The DIRDIF-99 Program System;* Technical Report of the Crystallography Laboratory; University of Nijmegen: Nijmegen, The Netherlands, 1999.

(13) *International Tables for Crystallography;* Kluwer Academic Publishers: Dordrecht, The Netherlands, 1992; Vol. C.

(14) *CrystalStructure 3.7.0*, *Crystal Structure Analysis Package*; Rigaku and Rigaku/MSC: The Woodlands, TX, 2000−2005.

(15) Watkin, D. J.; Prout, C. K.; Carruthers, J. R.; Betteridge, P. W. *CRYSTALS*, issue 10; Chemical Crystallography Laboratory: Oxford, U.K.